Existence of c-Kit negative cells with ultrastructural features of interstitial cells of Cajal in the subserosal layer of the *W/Wᵛ* mutant mouse colon

Hiromi Tamada and Hiroshi Kiyama

Department of Functional Anatomy and Neuroscience, Nagoya University, Graduate School of Medicine, Aichi, Japan

Abstract

Interstitial cells of Cajal (ICC) are mesenchymal cells that are distributed along the gastrointestinal tract and function as pacemaker cells or intermediary cells between nerves and smooth muscle cells. ICC express a receptor tyrosine kinase c-Kit, which is an established marker for ICC. The *c-kit* gene is allelic with the murine white-spotting locus (*W*), and some ICC subsets were reported to be missing in heterozygous mutant *W/Wᵛ* mice carrying *W* and *Wᵛ* mutated alleles. In this study, the characterization of interstitial cells in the subserosal layer of *W/Wᵛ* mice was analyzed by immunohistochemistry and electron microscopy. In the proximal and distal colon of *W/Wᵛ* mutant mice, no c-Kit-positive cells were detected in the subserosal layer by immunohistochemistry. By electron microscopy, the interstitial cells, which were characterized by the existence of caveolae, abundant mitochondria and gap junctions, were observed in the *W/Wᵛ* mutant colon. The morphological characteristics were comparable to those of the multipolar c-Kit positive ICC seen in the subserosa of proximal and distal colon of wild-type mice. Fibroblasts were also located in the same layers, but the morphology of the fibroblasts was distinguishable from that of ICC in wild type mice or of ICC-like cells in *W/Wᵛ* mutant mice. Collectively, it is concluded that c-Kit-negative interstitial cells showing a typical ICC ultrastructure exist in the proximal and distal colon of *W/Wᵛ* mutant mice.

Key words: interstitial cells of Cajal, subserosa, *W/Wᵛ* mutant mice, c-Kit, ultrastructure

Introduction

Interstitial cells of Cajal (ICC) are localized along the digestive tract and play important roles in normal gastrointestinal motility, including peristalsis. ICC primarily function as pacemaker cells or intermediary cells

Corresponding author: Hiroshi Kiyama, Department of Functional Anatomy & Neuroscience, Nagoya University, Graduate School of Medicine, 65 Tsurumaicho, Showaku, Nagoya, Aichi 466-8550, Japan
Phone: +81-52-744-2015 Fax: +81-52-744-2027 e-mail: kiyama@med.nagoya-u.ac.jp

between nerves and smooth muscle cells. ICC are divided into several subtypes based on their histological localization, and have different functions and morphological features (1–3). For example, the ICC associated with the myenteric plexus (ICC-MP) are pacemaker cells while the ICC within the circular and longitudinal muscle layers, respectively are intermediary cells. In addition to these major subtypes, there are some specific types within certain layers of the intestine, such as the ICC associated with the deep muscular plexus (ICC-DMP) in the small intestine (4), the ICC associated with the submuscular plexus in the colon (5, 6), and the ICC in the subserosal layer of the colon (ICC-SS) (3, 7, 8). The characteristic ultrastructure of ICC is the existence of caveolae, intermediate filaments, well-developed mitochondria, a basal lamina, and large gap junctions between cells. The c-Kit receptor tyrosine kinase, whose natural ligand is stem cell factor (SCF), is expressed on the cell surface of ICC, and is an established marker for immunohistochemical identification of these cells (9, 10).

The *c-kit* gene is allelic with the murine white-spotting locus (*W*) (11, 12). To date, several mutations in the *W* locus have been identified (*W*, W^{37}, W^v, W^{55}, W^{41}, W^{44}, and W^{57}), and a heterozygote for two distinct mutations, *W* and W^v (*W/W^v*) are frequently used as tools for ICC analysis (13, 14). The *W* mutation involves deletion of the transmembrane domain of c-Kit, while W^v is a point mutation in the kinase domain of c-Kit (15). *W/W^v* mutant mice are able to mature into adult mice, but show disorders of pacemaker activity in the intestine through a deficit of ICC-MP in the small intestine (16). Intriguingly, not all subtypes of ICC disappear in *W/W^v* mutant mice, and the subtypes that remain may have a lower dependency on c-Kit/SCF activity during development (17). For instance, ICC-MP in the small intestine of *W/W^v* mutant mice disappear, while ICC-MP in the proximal colon remain. Regarding ICC in the muscle layers, these cells exist in the small intestine of *W/W^v* mutant mice, but disappear in the stomach of these mice.

These ICC subtype-dependent losses in *W/W^v* mutant mice would be advantageous for analyzing the functions of the ICC subtypes, and therefore comprehension of the precise localization of ICC subtypes in *W/W^v* mutant mice would be crucial. One of the subtypes that has not been explored yet in *W/W^v* mutant mice is ICC-SS. ICC-SS, which are localized in the mouse colon, are identified by their morphology (3, 8), but the functional role of ICC-SS remains unclear. In this study, we focused on cells located in the subserosal layer of *W/W^v* mutant mice, and demonstrated two types of c-Kit negative interstitial cells via immunohistochemistry and electron microscopy.

Materials and Methods

Animals

WBB6F1/Kit-Kit^w/Kit^{w-v}/Slc and C57BL/6NcrSlc mice at 5–7 weeks of age were purchased from Japan SLC. The use and treatment of the animals followed the guidelines for animal experiments of Nagoya University. A segment of proximal colon approximately 2 cm in length was removed from the junction between the caecum and colon, while the distal colon segment was removed just anterior to the rectum.

Immunohistochemistry

Short segments of the proximal and distal colon were removed, briefly rinsed in 0.01 M phosphate-buffered saline (PBS), fixed for 20 min in acetone at 4°C, and washed in PBS. To obtain cryosections, the specimens were cut into small pieces, immersed in sucrose solutions, embedded in OCT compound (Sakura Finetek, Torrance, Calif., USA), and frozen. Cryosections with a thickness of 14–16 μm were obtained using a cryostat and mounted on MAS- coated glass slides.

To produce whole-mount stretch preparations, the mucosa, submucosa and muscle layer were peeled off. Isolated subserosal layers were placed in PBS containing 0.3% Triton X-100 for 20 min, and then preincubated in 4% Block Ace solution (DS Pharma Biomedical, Osaka, Japan) for 20 min. The specimens were subsequently incubated with a monoclonal rat anti-mouse CD117 antibody (c-Kit; ACK2; 1:200; eBioscience, Calif., USA) to label ICC, a rabbit anti-human PGP9.5 antibody (1:500; Ultraclone, Yarmouth, UK) to label the nervous components, and a rabbit anti-platelet-derived growth factor receptor α (PDGFRα) antibody (1:1000; Cell Signaling, Danvers, Mass., USA) to label the fibroblasts. Next, the specimens were incubated with secondary antibodies conjugated with Alexa 488 (goat anti-rat IgG; 1:500; Invitrogen, Eugene, Oregon, USA) or Alexa 594 (goat anti-rabbit IgG; 1:500; Invitrogen). The specimens were observed under a fluorescence microscope (BX23; Olympus, Tokyo, Japan).

Electron microscopy

Short segments of the proximal and distal colon were placed in a fixative containing 3% glutaraldehyde and 4% paraformaldehyde in 0.1 M phosphate buffer for 3–4 h at 4°C. The specimens were then rinsed in the same buffer, post-fixed in 1% osmium tetroxide in the same buffer for 2 h at 4°C, rinsed with distilled water, block-stained overnight in a saturated solution of uranyl acetate, dehydrated in an ethyl alcohol series, and embedded in epoxy resin.

Following examination of semi-thin sections stained with toluidine blue to select suitable areas, ultrathin sections were cut using an ultramicrotome (UC7k; Leica Microsystems, Wetzlar, Germany). The sections were then double-stained with uranyl acetate and lead citrate, and processed for observation with a transmission electron microscope (JEM-1400EX; JEOL, Tokyo, Japan).

Results

In the proximal colon of wild-type mice, c-Kit-immunoreactivity observed in whole-mount preparations revealed multipolar ICC-SS (Fig. 1a). These cells were apparently distinguishable from the bipolar ICC within the longitudinal muscle layers. In the subserosal layer, fibroblasts positive for PDGFRα were also observed as multipolar cells (Fig. 1a). In longitudinal sections, c-Kit-positive ICC were observed in the subserosal layer and myenteric plexus layer, identified by staining for the neuronal marker PGP9.5 (Fig. 1b). A similar localization pattern of c-Kit-positive cells (ICC-SS and ICC-MP) was observed in the distal colon of wild-type mice (Fig. 1c and d). In the proximal and distal colon of *W/Wᵛ* mutant mice, no c-Kit-positive cells were identified in the subserosal layer, while the fibroblast localization was similar to that observed in wild-type mice (Fig. 1e and g). In cryosections of the proximal colon, c-Kit-immunoreactive ICC-MP, which are already known to exist in *W/Wᵛ* mutant mice, were observed, but no c-Kit-positive cells were identified in the subserosal layer (Fig. 1f). In cryosections of the distal colon in *W/Wᵛ* mutant mice, no detectable c-Kit-positive cells were observed in either the subserosa or myenteric plexus (Fig. 1h).

Under electron microscopic observation, ICC as well as nerve fibers were identified in the connective tissue containing abundant collagen fibers between the longitudinal muscle layer and the subserosal mesothelial cells of the proximal colon (Fig. 2a). These cells had the typical ultrastructural characteristics of ICC, i.e. abundant mitochondria and caveolae (Fig. 2b). However, they did not have a basal lamina, which is one of the characteristics of ICC-SS in guinea pigs. In the distal colon, ICC were also observed in the subserosal layer (Fig. 2c and d). They could be distinguished from fibroblasts distributed in the same layer, because the fibroblasts had a well-developed rough endoplasmic reticulum and did not contain caveolae (Fig. 2e and f). Similarly, ICC-SS
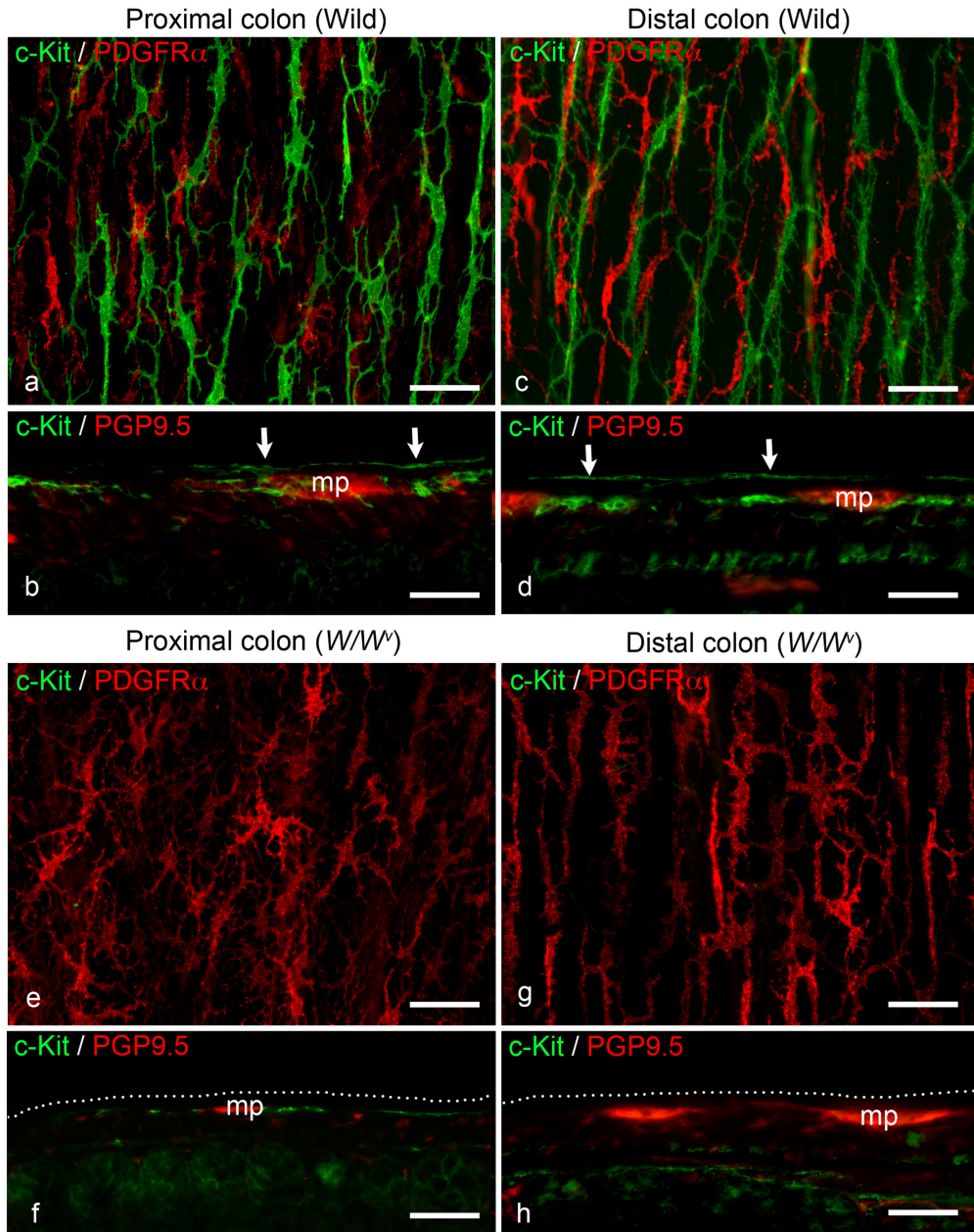
Fig. 1. **a** Whole-mount stretch preparation of the subserosal layer stained with anti-c-Kit (green) and anti-PDGFRα (red) antibodies in the wild-type proximal colon. Multipolar ICC (green) and fibroblasts (red) are distributed in the subserosal layer. **b** Longitudinal cryostat section of the wild-type proximal colon stained with anti-c-Kit (green) and anti-PGP9.5 (red) antibodies. ICC are present in the subserosal layer (arrows) and around the myenteric plexus (mp). **c** Whole-mount stretch preparation of the subserosal layer in the wild-type distal colon stained with the same antibodies as in (a). Similar findings are observed relative to the proximal colon. **d** Longitudinal section of the wild-type distal colon stained with the same antibodies as in (b). Similar findings are observed relative to the proximal colon. mp: myenteric plexus; arrows: ICC-SS. **e** Whole-mount stretch preparation of the subserosal layer in the *W/W^v* mouse proximal colon stained with the same antibodies as in (a). There are no c-Kit-positive ICC, but multipolar fibroblasts (red) are present in the subserosal layer. **f** Longitudinal section of the *W/W^v* mouse proximal colon stained with the same antibodies as in (b). ICC around the myenteric plexus (mp) can be observed, similar to the wild-type colon. There are no c-Kit-positive cells along the subserosal layer (dotted line). **g** Whole-mount stretch preparation of the subserosal layer in the *W/W^v* mouse distal colon stained with the same antibodies as in (a). Similar findings are observed relative to the proximal colon of *W/W^v* mice. **h** Longitudinal section of the *W/W^v* mouse distal colon stained with the same antibodies as in (b). No c-Kit-positive cells are observed in either the subserosa or myenteric plexus (mp). dotted line: subserosal layer. *Scale bar:* 50 µm.
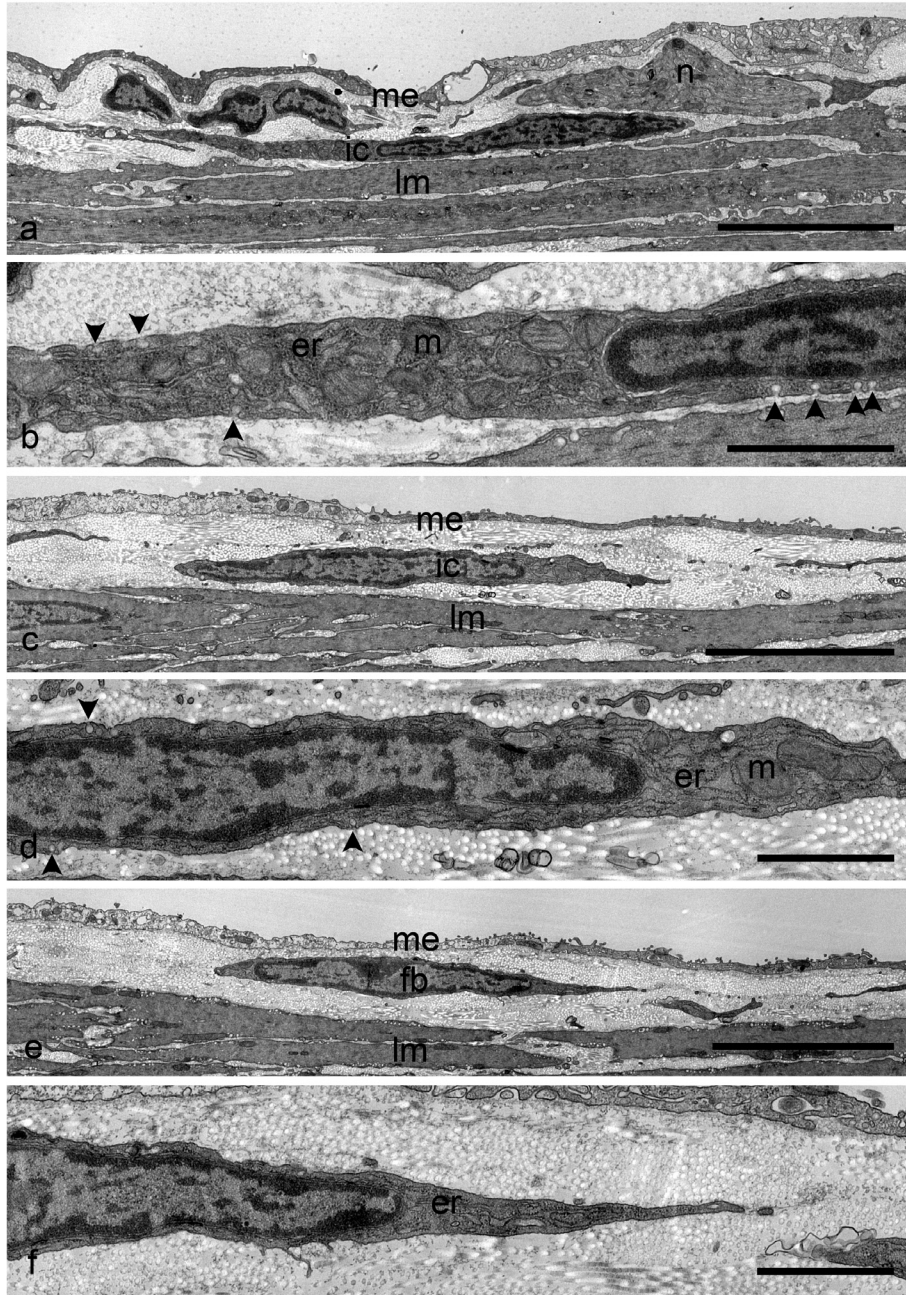
Fig. 2. **a** Electron micrograph showing ICC-SS in the wild-type proximal colon. ICC-SS (ic) are located in the narrow connective tissue space between the serosal mesothelium (me) and the longitudinal muscles (lm). Nerve bundles (n) are observed near the ICC-SS. **b** Higher magnification of the same ICC-SS shown in (a). The paranuclear cytoplasm contains mitochondria (m) and rough endoplasmic reticulum (er). Note the caveolae (arrowheads) along the cell membrane. **c** Electron micrograph showing ICC-SS in the wild-type distal colon. ICC (ic) are distributed just beneath the mesothelial cells (me). lm: longitudinal muscle. **d** Higher magnification of the same ICC-SS shown in (c). Mitochondria (m), caveolae (arrowheads), and rough endoplasmic reticulum (er) are detected. **e** Electron micrograph showing fibroblasts in the wild-type distal colon. Fibroblasts (fb) are also located in the narrow connective tissue space between the serosal mesothelium (me) and the longitudinal muscles (lm). **f** Higher magnification of the same fibroblasts shown in (e). The fibroblasts possess a well-developed rough endoplasmic reticulum (er). There are no caveolae on the cell surface. *Scale bars:* a, c, e, 5 µm; b, d, f, 1 µm.
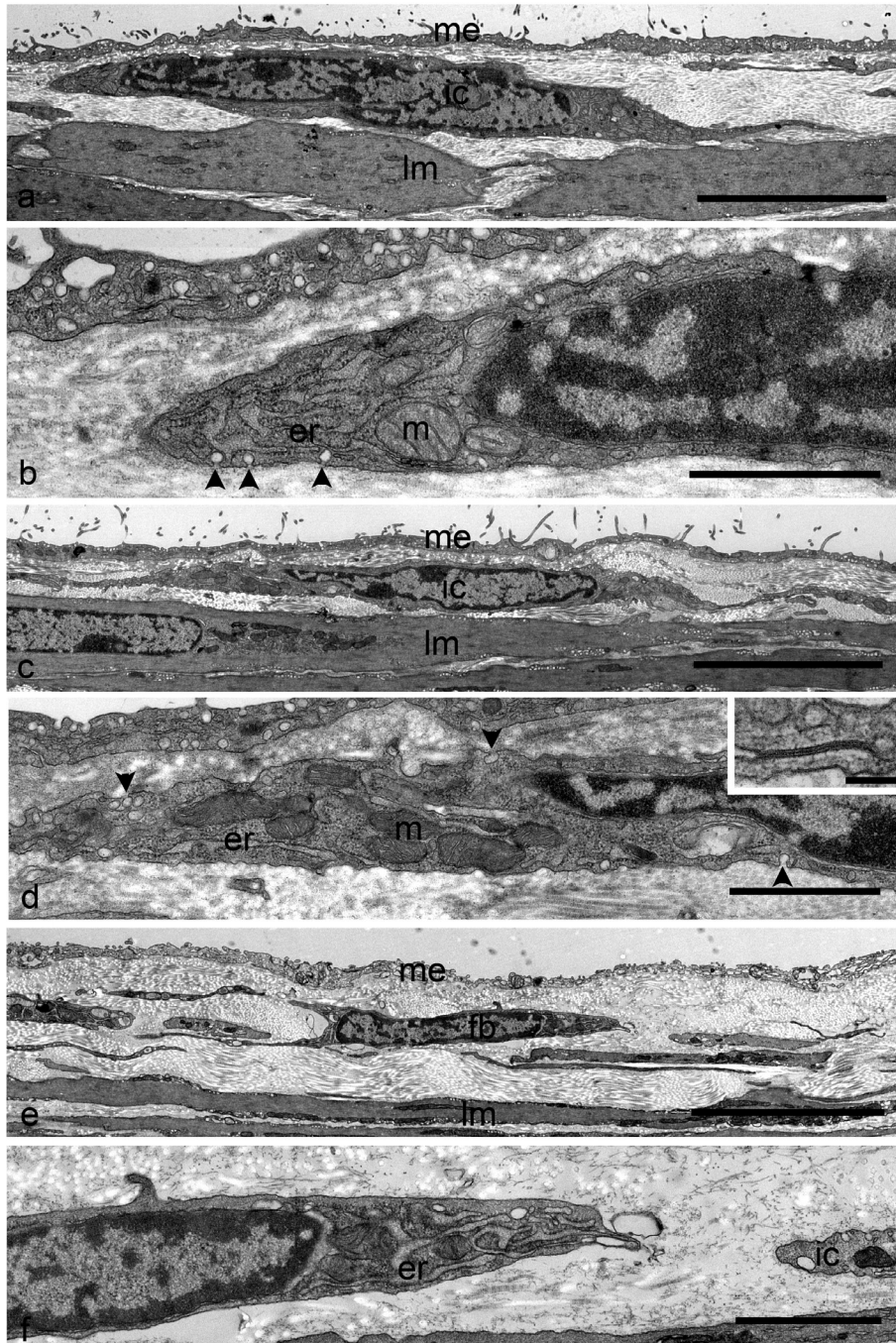
Fig. 3. **a** Electron micrograph showing interstitial cells with the ultrastructural features of ICC in the subserosal layer of the *W/W^v* mouse proximal colon. This interstitial cells (ic) are located in the narrow connective tissue space between the serosal mesothelium (me) and the longitudinal muscles (lm). **b** Higher magnification of the same cells shown in (a). The paranuclear cytoplasm contains mitochondria (m) and rough endoplasmic reticulum (er). Note the caveolae (arrowheads) along the cell membrane. **c** Electron micrograph showing interstitial cells with the ultrastructure of ICC in the subserosal layer of the *W/W^v* mouse distal colon. ICC (ic) are distributed just beneath the mesothelial cells (me). lm: longitudinal muscle. **d** Higher magnification of the same cells shown in (c). Mitochondria (m), caveolae (arrowheads), and rough endoplasmic reticulum (er) are detected. *Inset* Gap junction observed between the thin processes of these cells. **e** Electron micrograph showing fibroblasts in the *W/W^v* mouse proximal colon. Fibroblasts (fb) are also located in the narrow connective tissue space between the serosal mesothelium (me) and the longitudinal muscles (lm). **f** Higher magnification of the same fibroblasts shown in (e). The fibroblasts possess a well-developed rough endoplasmic reticulum (er). There are no caveolae on the cell surface. A fraction of interstitial cells (ic) with caveolae can be observed. *Scale bars:* a, c, e, 5 μm; b, d, f, 1 μm; d *Inset* 100 nm.

were distinguished from smooth muscle cells, which contained contractile filaments.

Ultrastructural examination of the proximal colon of *W/W^v* mutant mice revealed two types of interstitial cells which were located in the subserosal layer (Fig. 3a, b, e, and f). These were also identified in the distal colon (Fig. 3c and d). One type showed typical fibroblast morphology (Fig. 3e and f), and the other had apparently similar ultrastructure to ICC seen in the wild-type colon, which had cells characterized by abundant mitochondria and caveolae (Fig. 3a, b, c, and d). In addition, the processes of the latter type were connected with each other via gap junctions (Fig.3d *Inset*). This type of cell was readily distinguishable from smooth muscle cells and the former interstitial cell, which had typical characteristics of fibroblast ultrastructure. These observations indicated that c-Kit-negative interstitial cells in the subserosal layer of the proximal and distal colon in *W/W^v* mutant mice possessed the ultrastructural features of ICC.

Discussion

In this study, we have identified two types of interstitial cells in the colon of *W/W^v* mutant mice, and demonstrated their morphological characteristics. Both the proximal and distal colon of wild-type mice contained c-Kit-positive cells, which were assumed to correspond to ICC-SS in guinea-pigs (7), and the ultrastructure of these cells demonstrated the typical characteristics of ICC, such as abundant mitochondria, and caveolae, but no basal lamina. They were different from fibroblasts, which were characterized by well-developed rough endoplasmic reticulum and no caveolae.

In the colon of *W/W^v* mutant mice, c-Kit-immunoreactive cells were not observed in the subserosal layer, whereas the fibroblast localization in this layer appeared similar to that seen in wild-type mice. However, electron microscopic observation revealed the apparent existence of the other interstitial cell, which was characterized by caveolae, abundant mitochondria, and gap junctions in the subserosal layer, suggesting that this cell in *W/W^v* mutant mice and the ICC-SS in the wild type colon were morphologically identical. The existence of the nerve fibers near ICC-SS in the proximal colon was demonstrated by Vanderwinden (8) and also in this electron microscopic study of the wild type colon. Under fluorescent microscopy observation, the nerve density in the subserosal layer of both the wild type and *W/W^v* colon were comparable (data not shown). This suggests that the interstitial cells in *W/W^v* mutant mice and ICC-SS in wild type also have a similar innervation. In previous studies, impairment of c-Kit-mediated signaling by injection of a neutralizing monoclonal antibody (ACK2) after birth disturbed both ICC development and normal contractile activity of the intestine (18, 19). Another report showed that mesenchymal precursors, which give rise to smooth muscle cells, differentiated into ICC when Kit-mediated signaling was activated in the embryo (20). Therefore, it has been assumed that Kit/SCF signaling is crucial for proper ICC development. However, some ICC, such as ICC-MP in the small intestine, are reported to develop even with low Kit/SCF activity. Additionally, the survival of ICC-DMP in *W/W^v* mutant mice has been reported (21, 22), and several studies show that interstitial cells corresponding to ICC-DMP can be detected even when there were no c-Kit positive cells in the deep muscular plexus of *W* mutant animals (23, 24). In this context, the c-Kit-dependency of the ICC in the subserosa may be lower and comparable to the dependency of ICC-MP in the proximal colon and ICC-DMP in the small intestine (17). If they are the same cells as ICC-SS in the wild type colon, it is unclear why the interstitial cells in this study do not express c-Kit receptors. The specific conditions, in which they have a sparse innervation as compared with ICC-DMP in the deep muscular plexus, may make them c-Kit negative rather than c-Kit positive ICC-DMP even in the *W/W^v* colon.

Although c-Kit is the most reliable marker at present, recently some papers suggest the using of Ano1 as a more suitable marker for ICC (25). Further studies of ICC are needed to explore other markers for detecting

ICC, especially in *W* mutant mice.

In conclusion, c-Kit negative interstitial cells with an ultrastructure corresponding to that of c-Kit+ ICC-SS found in wild type mice, exist in the subserosal layer of the colon of *W/W^v* mutant mice. Further studies are needed to reveal the roles of both ICC-SS in wild-type mice and the c-Kit-negative interstitial cells in *W/W^v* mutant mice.

Acknowledgments

Conflict of interest

The authors declare that they have no conflict of interest.

Reference

1. Komuro T. Atlas of interstitial cells of Cajal in the gastrointestinal tract. Dordrecht (NL): Springer; 2012. 134p.

2. Sanders KM, Ward SM, Koh SD. Interstitial cells: regulators of smooth muscle fuction. Physiol Rev. 2014; 94(3): 859–907.

3. Thuneberg L. Interstitial cells of Cajal: intestinal pacemaker cells? Adv Anat Embryol Cell Biol. 1982; 71: 1–130.

4. Rumessen JJ, Mikkelsen HB, Thuneberg L. Ultrastructure of interstitial cells of Cajal associated with deep muscular plexus of human small intestine. Gastroenterology. 1992; 102(1): 56–68.

5. Plujà L, Albertí E, Fernández E, Mikkelsen HB, Thuneberg L, Jiménez M. Evidence supporting presence of two pacemakers in rat colon. Am J Physiol Gastrointest Liver Physiol. 2001; 281(1): 255–66.

6. Smith TK, Reed JB, Sanders KM. Interaction of two electrical pacemakers in muscularis of canine proximal colon. Am J Physiol. 1987; 252(3 Pt 1): 290–9.

7. Aranishi H, Kunisawa Y, Komuro T. Characterization of interstitial cells of Cajal in the subserosal layer of the guinea-pig colon. Cell Tissue Res. 2009; 335(2): 323–9.

8. Vanderwinden JM, Rumessen JJ, Bernex F, Schiffmann SN, Panthier JJ. Distribution and ultrastructure of interstitial cells of Cajal in the mouse colon, using antibodies to Kit and *Kit^{W-lacZ}* mice. Cell Tissue Res. 2000; 302(2): 155–70.

9. Burns AJ, Herbert TM, Ward SM, Sanders KM. Interstitial cells of Cajal in the guinea-pig gastrointestinal tract as revealed by c-Kit immunohistochemistry. Cell Tissue Res. 1997; 290(1): 11–20.

10. Torihashi S, Nishi K, Tokutomi Y, Nishi T, Ward S, Sanders KM. Blockade of kit signaling induces transdifferentiation of interstitial cells of cajal to a smooth muscle phenotype. Gastroenterology. 1999; 117(1): 140–8.

11. Chabot B, Stephenson DA, Chapman VM, Besmer P, Bernstein A. The proto-oncogene *c-kit* encoding a transmembrane tyrosine kinase receptor maps to the mouse *W* locus. Nature. 1988; 335(6185): 88–9.

12. Geissler EN, Ryan MA, Housman DE. The dominant-white spotting (*W*) locus of the mouse encodes the *c-kit* proto-oncogene. Cell. 1988; 55(1): 185–92.

13. Huizinga JD, Thuneberg L, Klüppel M, Malysz J, Mikkelsen HB, Bernstein A. *W/kit* gene required for interstitial cells of Cajal and for intestinal pacemaker activity. Nature. 1995; 373 (6512): 347-9.

14. Ward SM, Burns AJ, Torihashi S, Sanders KM. Mutation of the proto-oncogene c-kit blocks development of interstitial cells and electrical rhythmicity in murine intestine. J Physiol. 1994; 480(Pt 1): 91–7.

15. Nocka K, Tan JC, Chiu E, Chu TY, Ray P, Traktman P, Besmer P. Molecular bases of dominant negative and loss of function mutations at the murine c-kit/white spotting locus: W37, Wv, W41 and W. EMBO J. 1990; 9(10): 1805–13.

16. Kitamura Y, Hirota S, Nishida T. A loss-of-function mutation of *c-kit* results in depletion of mast cells and interstitial cells of Cajal, while its gain-of-function mutation results in their oncogenesis. Mutat Res. 2001; 477(1–2): 165–71.

17. Iino S, Horiguchi S, Horiguchi K, Nojyo Y. Interstitial cells of Cajal in the gastrointestinal musculature of W mutant mice. Arch Histol Cytol. 2007; 70(3): 163–73.

18. Torihashi S, Ward SM, Nishikawa S, Nishi K, Kobayashi S, Sanders KM. c-kit-dependent development of interstitial cells and electrical activity in the murine gastrointestinal tract. Cell Tissue Res. 1995; 280(1): 97–111.

19. Torihashi S, Ward SM, Sanders KM. Development of c-Kit-positive cells and the onset of electrical rhythmicity in murine small intestine. Gastroenterology. 1997; 112(1): 144–55.

20. Maeda H, Yamagata A, Nishikawa S, Yoshinaga K, Kobayashi S, Nishi K, Nishikawa S. Requirement of c-kit for development of intestinal pacemaker system. Development. 1992; 116(2): 369–75.

21. Iino S, Horiguchi K, Horiguchi S, Nojyo Y. c-Kit-negative fibroblast-like cells express platelet-derived growth factor receptor alpha in the murine gastrointestinal musculature. Histochem Cell Biol. 2009; 131(6): 691–702.

22. Malysz J, Thuneberg L, Mikkelsen HB, Huizinga JD. Action potential generation in the small intestine of W mutant mice that lack interstitial cells of Cajal. Am J Physiol. 1996; 271(3 Pt 1): 387–99.

23. Horiguchi K, Komuro T. Ultrastructural characterization of interstitial cells of Cajal in the rat small intestine using control and *Ws/Ws* mutant rats. Cell Tissue Res. 1998; 293(2): 277–84.

24. Iino S, Horiguchi K, Nojyo Y. *W^{sh}/W^{sh}* c-Kit mutant mice posess interstitial cells of Cajal in the deep muscular plexus layer of the small intestine. Neurosci Lett. 2009; 459(3): 123–6.

25. Wang XY, Chen JH, Li K, Zhu YF, Wright GW, Huizinga JD. Discrepancies between c-Kit positive and Ano1 positive ICC-SMP in the *W/W^v* and wild-type mouse colon; relationships with motor patterns and calcium transients. Neurogastroenterol Motil. 2014; 26: 1298–310.